



High Expression of INF2 Predicts Poor Prognosis and Promotes Hepatocellular Carcinoma Progression*

WANG Hai-Biao^{1)**}, LIN Man^{3)**}, YE Fu-Sang⁴⁾, SHI Jia-Xin³⁾, LI Hong^{1,3)***},
 YE Meng^{2,3)***}, WANG Jie^{2)***}

¹⁾Department of Hepatobiliary and Pancreatic Surgery, Ningbo Medical Center of LiHuiLi Hospital, Ningbo 315040, China;

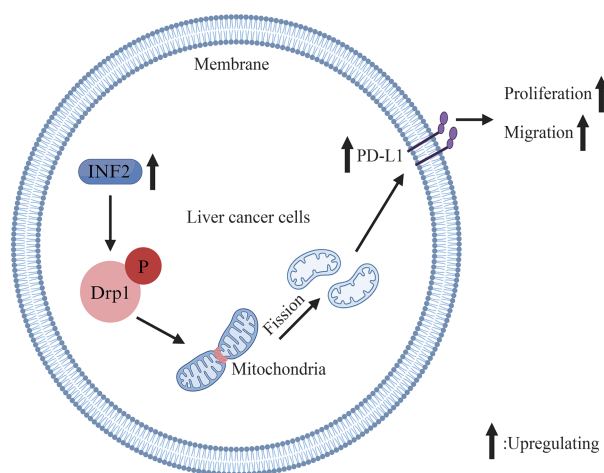
²⁾Department of Radiotherapy and Chemotherapy, The First Affiliated Hospital of Ningbo University, Ningbo 315010, China;

³⁾Department of Biochemistry and Molecular Biology, Zhejiang Key Laboratory of Pathophysiology, Science Health Center of Ningbo University, Ningbo 315211, China;

⁴⁾Department of Pathology, Ningbo Clinical Pathology Diagnosis Center, Ningbo 315021, China)

Abbreviations: HCC, hepatocellular carcinoma; INF2, inverted formin 2; TCGA, The Cancer Genome Atlas; TIMER2, tumor immune estimation resource, version 2; LIHC, liver hepatocellular carcinoma; IHC, immunohistochemistry; BCA, dicarboxylic acid; PVDF, polyvinylidene fluoride; HRP, horseradish peroxidase; DMEM, Dulbecco's Modified Eagle Medium; ANOVA One-way, analysis of variance; BLCA, bladder urothelial carcinoma; CHOL, cholangio carcinoma; ESCA, esophageal carcinoma; HNSC, head and neck squamous cell carcinoma; KIRC, kidney renal clear cell carcinoma; KIRP, kidney renal papillary cell carcinoma; STAD, stomach adenocarcinoma; THCA, thyroid carcinoma; UCEC, uterine corpus endometrial carcinoma; AP-MS, affinity purification and mass spectrometry; TIMP1: tissue inhibitor of metalloproteinase-1; LOX: lysyl oxidase; LOX2: lysyl oxidase-like 2.

Graphical abstract



* This work was supported by grants from the Natural Science Foundation of Ningbo (202003N4197), The Ningbo Health Technology Project (2022Y13), Ningbo Digestive System Tumor Clinical Medicine Research Center (2019A21003), Zhejiang Province Basic Public Welfare Research Plan (LTGY24H160004), the Medical and Health Project of Zhejiang Province (2022KY1079), Ningbo University Student Research and Innovation Program (2024SRIP1925), and the K. C. Wong Magna Fund of Ningbo University.

** These authors contributed equally to this work.

*** Corresponding author.

LI Hong. Tel: 86-574-87018651, E-mail: lancet2017@163.com

YE Meng. Tel: 86-574-87085337, E-mail: yemeng@nbu.edu.cn

WANG Jie. Tel: 86-574-87085337, E-mail: wangjiemedical@163.com

Received: April 9, 2024 Accepted: August 29, 2024

Abstract Objective INF2 is a member of the formins family. Abnormal expression and regulation of INF2 have been associated with the progression of various tumors, but the expression and role of INF2 in hepatocellular carcinoma (HCC) remain unclear. HCC is a highly lethal malignant tumor. Given the limitations of traditional treatments, this study explored the expression level, clinical value and potential mechanism of INF2 in HCC in order to seek new therapeutic targets. **Methods** In this study, we used public databases to analyze the expression of INF2 in pan-cancer and HCC, as well as the impact of INF2 expression levels on HCC prognosis. Quantitative real time polymerase chain reaction (RT-qPCR), Western blot, and immunohistochemistry were used to detect the expression level of INF2 in liver cancer cells and human HCC tissues. The correlation between INF2 expression and clinical pathological features was analyzed using public databases and clinical data of human HCC samples. Subsequently, the effects of INF2 expression on the biological function and Drp1 phosphorylation of liver cancer cells were elucidated through *in vitro* and *in vivo* experiments. Finally, the predictive value and potential mechanism of INF2 in HCC were further analyzed through database and immunohistochemical experiments. **Results** INF2 is aberrantly high expression in HCC samples and the high expression of INF2 is correlated with overall survival, liver cirrhosis and pathological differentiation of HCC patients. The expression level of INF2 has certain diagnostic value in predicting the prognosis and pathological differentiation of HCC. *In vivo* and *in vitro* HCC models, upregulated expression of INF2 triggers the proliferation and migration of the HCC cell, while knockdown of INF2 could counteract this effect. INF2 in liver cancer cells may affect mitochondrial division by inducing Drp1 phosphorylation and mediate immune escape by up-regulating PD-L1 expression, thus promoting tumor progression. **Conclusion** INF2 is highly expressed in HCC and is associated with poor prognosis. High expression of INF2 may promote HCC progression by inducing Drp1 phosphorylation and up-regulation of PD-L1 expression, and targeting INF2 may be beneficial for HCC patients with high expression of INF2.

Key words HCC, INF2, expression, prognosis, Drp1

DOI: 10.16476/j.pibb.2024.0151

CSTR: 32369.14.pibb.20240151

Primary liver cancer, a malignant cancer, of which 75%–85% of cases are hepatocellular carcinoma (HCC), is the sixth most common cancer and the third leading cause of cancer-related deaths worldwide^[1]. Although the causes of HCC, including obesity, cigarette smoking, excessive alcohol consumption, and hepatitis virus infection, are preventable, the 5-year survival rate of patients with HCC is far less than 20%^[2-3]. Advances in systemic therapy have resulted in remarkable therapeutic efficacy. However, chemoresistance and HCC recurrence can develop after treatment, leading to high mortality in HCC^[2, 4]. Therefore, identification of new therapeutic targets for HCC treatment is urgently required.

The liver, the major metabolic organ, regulates whole-body energy-related metabolism, including glucose, fatty acids, and amino acid metabolism. Notably, these metabolisms mainly occur in the mitochondria, which are abundant in the liver to ensure energy homeostasis^[5]. Mitochondria, the cell powerhouses, are intracellular double membrane-bound structures that play multiple roles in energy metabolism and cellular homeostasis, including in the regulation of oxidative stress, signal transduction,

metabolism, and cell apoptosis susceptibility, forming a complex organelle network in cytosol, which is balanced *via* the molecular events of dynamic fusion and fission^[6-9]. Mitochondrial dysfunction plays a crucial role in tumor transformation, and mitochondrial dynamics have been identified as key therapeutic targets for the treatment of cancer^[8].

Inverted formin 2 (INF2) is a vertebrate formin protein involved in actin-related and microtubule-related processes. In mammalian cells, there are two isoforms of INF2 that differ in their C-terminal sequence: the ER-binding prenylated (CAAX) isoform and the cytoplasmic nonCAAX isoform. INF2-CAAX induces actin filaments that may drive initial mitochondrial constriction, whereas INF2 mutations can lead to Charcot-Marie-Tooth disease. Suppression of INF2-nonCAAX in tissue culture cells can cause Golgi dispersal^[10-11]. Moreover, increasing evidence indicates that the abnormal expression and regulation of INF2 are associated with human cancers. For example, previous studies have shown that dysregulation of SPOP-mediated INF2 ubiquitination promotes mitochondrial fission, triggering prostate cancer^[12]. INF2 is overexpressed in basal-like breast cancers, and is important for the maintenance of cell

shape, migration, invasion, and proliferation^[13]. INF2 is upregulated in glioblastoma and endometrial carcinoma tissues, while knockdown of INF2 significantly reduces the migration of glioblastoma cells and endometrial cancer cell migration in most studied cell lines^[14-15]. Additionally, one study suggested that INF2-mediated mitochondrial fission plays a suppressive role in colorectal cancer, and IL-2-based therapy could increase INF2-related mitochondrial fission, triggering colorectal cancer cell apoptosis^[16]. Although INF2-related functions have been studied in several cancers, the role of INF2 in HCC remains unclear.

Here, we found that the mRNA level of *INF2* was higher in HCC samples from the database of The Cancer Genome Atlas (TCGA), as well as the protein level of INF2 in HCC patient' tissues tested by immunohistochemistry (IHC) assay. High INF2 expression in clinical HCC samples is associated with poor survival, and the high expression level of INF2 in HCC tissues is significantly related to liver cirrhosis and pathological differentiation from our clinical HCC tissues. Moreover, overexpression of INF2 (hereafter referred to INF2-CAAX) promoted the proliferation and migration of liver cancer cells, while INF2 knockdown significantly inhibited this phenomenon. Mechanistically, INF2-CAAX may play an oncogenic role in liver cancer *via* Drp1-mediated mitochondrial hyper-division. In summary, our results suggest a vital role of INF2 in the proliferation and migration of liver cancer cells; targeting INF2 may be a potential treatment strategy for HCC patients with high expression of INF2.

1 Materials and methods

1.1 Data collection

INF2 RNA levels and associated clinicopathological characteristics were obtained from TCGA. Differential expression and prognostic analyses were performed using R software (version 4.2.1). TIMER2 (Tumor Immune Estimation Resource, version 2) web (<http://timer.cistrome.org/>) was used to examine *INF2* gene expression among specific tumor subtypes and to investigate the relationship between INF2 expression and immune infiltrates in HCC. In addition, we obtained boxplots of INF2 expression in different tumor subgroups according to clinicopathological characteristics from

the UALCAN database (<http://ualcan.path.uab.edu>). Welch's *t*-test was used to evaluate differences.

1.2 Clinical specimens

The 69 pairs of human HCC tissue samples included in the study were collected and diagnosed with HCC by the Ningbo Clinical Pathology Diagnosis Center. Fifty formalin-fixed human HCC tissue samples were obtained from the Ningbo Clinical Pathology Diagnosis Center. The remaining 19 pairs of fresh human liver cancer tissue samples were obtained from Ningbo Medical Center of LiHuiLi Hospital. All patients signed an informed consent form before using the clinical materials. Clinical HCC samples were collected with the permission of the hospital's Human Ethics Committee (KY2020PJ135) and were limited to laboratory research.

1.3 Immunohistochemistry (IHC)

Fifty pairs of formalin-fixed HCC tissues were embedded in paraffin and cut into 4 μ m sections. Paraffin sections were stained for IHC to detect target protein expression. Paraffin sections were soaked sequentially with xylene and different ethanol concentrations to deparaffinize and rehydrate. Next, the antigen was retrieved at a high temperature using sodium citrate diluent. Finally, the slides were incubated with an anti-INF2 antibody (1 : 50, ABclonal, USA, Cat NO: A10038) or anti-PD-L1 antibody (1 : 1 000, proteintech, China, Cat NO: 28076-1-AP) at 4°C, and the secondary antibody was incubated with the standard avidin-biotin-labeled peroxidase complex method. DAB staining was used for target protein staining, and nucleus were counterstained with hematoxylin. Images were acquired using an upright microscope system (Nikon, Japan) after coverslipping. Two pathologists scored the positive degree of IHC staining and divided the patients into three groups with different scores. The immunohistochemical score was the sum of the staining intensity score and positive cell percentage score. Dyeing intensity score: no color, 0 points; light yellow, 1 point; yellow, 2 points; brown-yellow, 3 points. The percentage of positive cells: 0%–10%, 0 points; 11%–25%, 1 point; 26%–50%, 2 points; 51%–75%, 3 points; 75%–100%, 4 points. According to the immunohistochemical score, a total score of 0 classified as negative, 1–2 classified as low positive, 3–4 classified as positive, and 5–7 classified as high

positive.

1.4 Western blot (WB)

Total cell proteins were lysed using RIPA buffer containing protease inhibitors (Solarbio, China). The protein extract was harvested and quantified by bicinchoninic acid assay (BCA) analysis (Beyotime, China). The protein extract was separated using 10% SDS-PAGE and transferred to a polyvinylidene fluoride (PVDF) membrane (Millipore, USA). The membrane was incubated with a high affinity anti-INF2 antibody (1 : 1 000, ABclonal, USA, Cat NO: A10038), and then incubated with a secondary antibody conjugated with horseradish peroxidase (HRP) (1 : 1 000, Cell Signal Technology, USA). All quantifications were normalized to the protein level of the endogenous control, GAPDH (cat#A19056, Abclonal, China). After washing, the signal was detected using a chemiluminescence system (Bio-Rad, USA) and analyzed using ImageJ software.

1.5 Plasmid construction and transfection

INF2 cDNA was obtained from the total RNA sequences of HepG2 cells using specific primers and sub-cloned into the pCDH-Myc vector to construct the pCDH-Myc-INF2 plasmid. For lentiviral knockdown, the short hairpin RNA (shRNA) sequence targeting INF2 was sub-cloned into pCDH-GFP-shRNA vectors. All constructs were verified by DNA sequencing.

Transfections were performed using Lipo6000 TM transfection reagent (Beyotime, China, Cat No: C0526) according to the manufacturer's instructions. Liver cancer cells were seeded in a 6-well plate and transiently transfected with 3 μ g of pCDH-Myc-INF2 and shINF2 (INF2 knockdown) or an empty vector.

1.6 RT-qPCR

According to the kit instructions, total RNA was extracted from HepG2 cells by RNA Easy Fast Tissue/Cell Kit (Catalog: DP451, Tiangen, Beijing, China). RNA quality was measured using a SpectraMax® QuickDrop™ (Molecular Devices, Sunnyvale, CA, United States). Next, reverse transcription of 1 μ g of total RNA was performed using the FastKing gDNA Dispelling RT SuperMix (Catalog: KR118-02, Tiangen, Beijing, China). The following primer pairs were applied for the quantitative real time polymerase chain reaction (RT-qPCR): INF2 forward, 5'-CTCTGGCCGTTGCCTCAC-3' and reverse, 5'-GCGTTGATCACGCTAAGCAG-3'; GAPDH forward, 5'-CA-

TGGCCTTCCGTGTTCCCTA-3' and reverse, 5'-CCC-TCAGATGCCTGCTTCA-3'. RT-qPCR reactions were prepared with Real Universal SYBR Green Premix (Catalog: FP201, Tiangen, Beijing, China) following the manufacturer's instructions. Reactions were carried out and data were analyzed using a LightCycler96 (Roche, Mannheim, Germany). The $2^{-\Delta\Delta Cq}$ method was used to analyze the expression of the target gene INF2. The experiment was independently repeated three times. GraphPad Prism 7 software was used for graphing and statistical analysis. Student's *t*-test was used for statistical analysis.

1.7 Cell culture

The human liver cancer cell lines HepG2 and Huh7 with a short tandem repeat (STR) identification certificate were obtained from the Shanghai Institute of Biochemistry and Cell Biology, Chinese Academy of Sciences. The cells were cultured in Dulbecco's Modified Eagle Medium (DMEM, Meilunbio, China, Cat No: MA0212-2) containing 10% fetal bovine serum (FBS, Standard Quality, OriCell, China, Cat No: FBSST-01033) and 1% penicillin/streptomycin (Catalog: 15140-122, Gibco). All cells were cultured in a humidified incubator at 37°C with 5% CO₂.

1.8 Colony formation assay

For the colony formation assay, transfected cells were seeded into 6-well plates at a density of 1 000/well and maintained in DMEM containing 10% FBS for two weeks. After being fixed with methanol, the cells were stained with 0.1% crystal violet for 30 min, and the colonies were imaged and counted.

1.9 Methyl thiazolyl tetrazolium (MTT) assay

For the MTT assay, transfected cells were seeded into 96-well plates at a density of 2 000/well. At 24, 48, 72, and 96 h after seeding, cell viability was measured using the MTT Cell Proliferation and Cytotoxicity Assay Kit (Solarbio, China) according to the manufacturer's instructions. Briefly, each well was added with 10 μ l MTT solution, and the plate was incubated at 37°C for 4 h in the dark. The absorbance was measured at 490 nm using a microplate reader (Tecan, Switzerland).

1.10 Wound-healing assay

The cells were seeded in a 6-well plate at a density of 2×10^5 /well. Two hours prior to scratching, cells were treated with 5 mg/L mitomycin C (S8146, Sigma) to control for differences in proliferation.

Scratches were produced at the tip of a sterile 200 μ l pipette, and the floating cells were cleaned with 1 \times phosphate buffer saline (PBS). Scratches were photographed at 0, 24, and 48 h after scratching using an inverted microscope.

1.11 Transwell migration assay

Cell migration was analyzed by Transwell. Using a 24-well Transwell chamber, 500 μ l culture medium containing 10% fetal bovine serum was added to the lower chamber, and 5 \times 10⁴ cells were placed in 150 μ l serum-free medium. After incubation at 37°C for 48 h, the cells on the upper surface of the membrane were scraped off. Invasive cells on the membrane surface were fixed with paraformaldehyde and stained with 0.5% crystal violet (Solarbio, China). Less than 5 random 200 \times micro-visual fields/hole were photographed and counted using a Nikon inverted microscope.

1.12 Cell cycle assay

3 \times 10⁶ cells were collected, and washed with PBS. The DNA staining solution and permeabilization solution were added to the cell suspension, mixed well, and allowed to stand away from light at room temperature for 30 min. Cells were assessed by flow cytometry (Becton Dickinson, USA), and the cell cycle was analyzed using the Cell Quest ModFit software.

1.13 *In vivo* xenograft assay

We examined the effects of INF2 overexpression or knockdown on HCC growth and metastasis *in vivo* xenograft assay. Four- to six-week-old NOD-SCID mice (strain No. T001492, Nanjing, China) were used to study the role of xenografted cells in a living organism. After one week of feeding under suitable conditions, four mice were randomly assigned to each group. Huh7 cells stably expressing control, INF2-OE, or shINF2#3 were injected subcutaneously into mice. The tumor size was measured with vernier calipers every 4 d, and the volume was calculated as $V = (\text{length} \times \text{width}^2) \times 1/2$. On the 20th day after injection, the mice were euthanized, and the subcutaneous tumors were isolated and photographed. All animal procedures were performed according to protocols approved by the Animal Care Committee of Ningbo University (AEWC-NBU20210295).

1.14 Statistical analysis

Analyses were performed using the SPSS software (version 20.0; SPSS, Inc., USA). Student's

paired *t*-tests were used to analyze the statistical significance of the differences between HCC and paratumor tissues. One-way analysis of variance (ANOVA) was used to determine the statistical significance of the differences among the different experimental groups. $P < 0.05$ was considered to indicate statistical significance.

2 Results

2.1 INF2 is upregulated in HCC and associated with poor prognosis

We applied the TIMER2 approach to analyze the expression levels of INF2 across various cancer types. The expression levels of INF2 in the tumor tissues of bladder urothelial carcinoma (BLCA), cholangiocarcinoma (CHOL), esophageal carcinoma (ESCA), head and neck squamous cell carcinoma (HNSC), kidney renal clear cell carcinoma (KIRC), kidney renal papillary cell carcinoma (KIRP), liver hepatocellular carcinoma (LIHC), stomach adenocarcinoma (STAD), thyroid carcinoma (THCA), uterine corpus endometrial carcinoma (UCEC) were higher than those in the corresponding normal tissues (Figure 1a). Furthermore, we explored the expression levels of INF2 in HCC and normal tissues using the TCGA databases. Similarly, the expression level of INF2 in HCC tissues was higher than that in the normal liver tissues (Figure 1b, c). In addition, the expression of INF2 in human liver hepatic stellate cell line LX-2 cells and human liver cancer cell lines HepG2, PLC and Huh7 cells was detected by RT-qPCR. The results showed that INF2 was highly expressed in human liver cancer cell lines compared with the human liver hepatic stellate cell line LX-2 cells (Figure S1).

Considering that there are no public databases for the protein level of INF2 in HCC, we investigated its protein expression profiles in HCC using WB to detect the protein level of INF2 in 19 pairs of HCC and its corresponding paratumor tissues. Although a high protein level of INF2 was observed in HCC tissues, due to the limited number of patients, the difference was not statistically significant (Figure 1d). Since fresh tissue samples came from hospitals and were limited by the amount of surgery, the number of specimens was extremely difficult to accumulate. To address this issue, we collected formalin-fixed tissue specimens originating from the Pathology Diagnostic

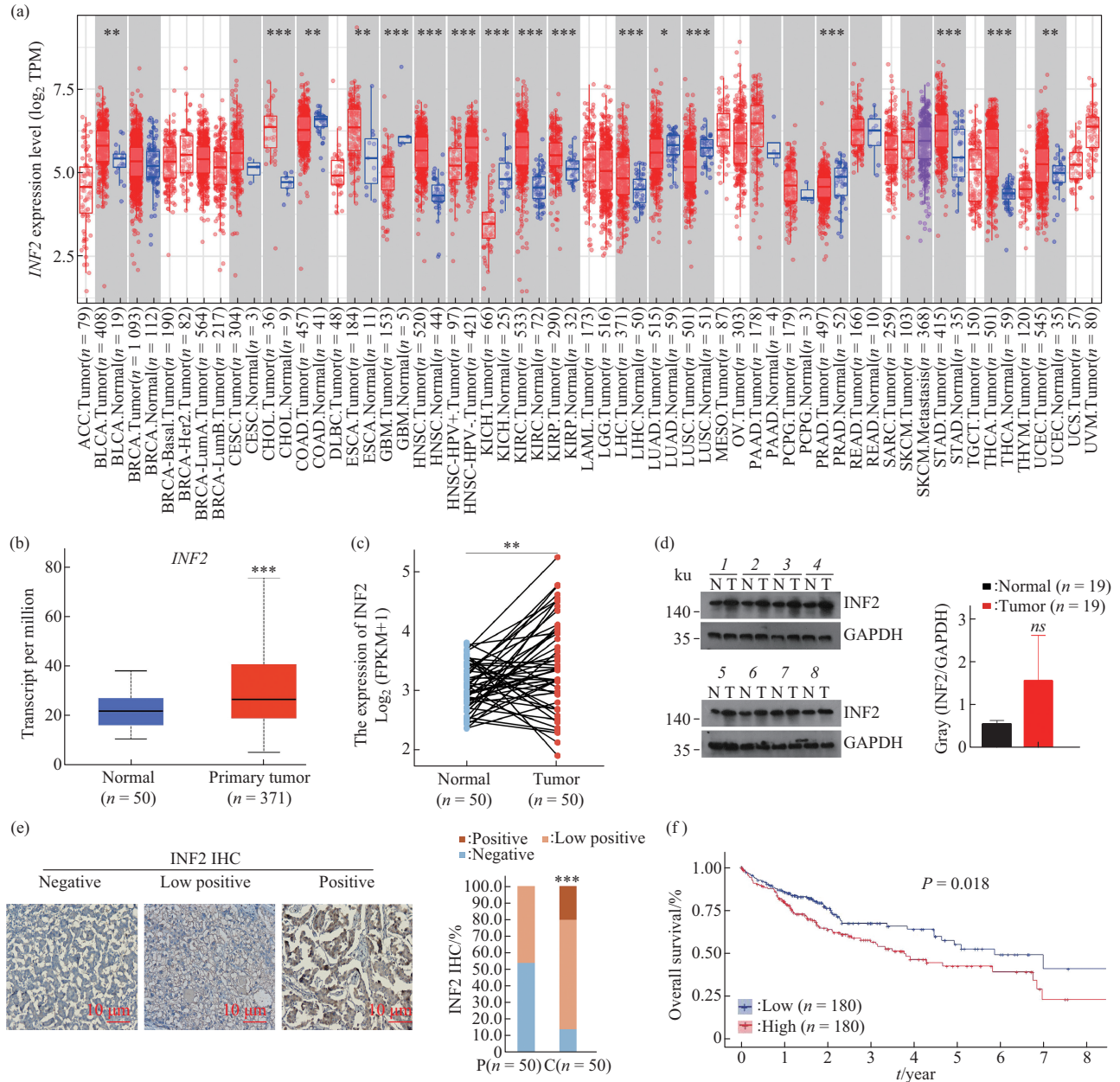


Fig. 1 *INF2* is upregulated in HCC and is associated with poor prognosis

(a) The expression status of the *INF2* gene in different cancers or specific cancer subtypes was analyzed through TIMER2. TPM: transcripts per million. (b) TCGA database analyses showed a higher level of *INF2* in HCC tissues than that in normal tissues. (c) *INF2* expression is higher in HCC than that in paired normal tissues. FPKM: fragments per kilobase of transcript per million mapped reads. (d) WB analyses of the expression of *INF2* in HCC and corresponding paratumor tissues at protein level (n=19). GAPDH was tested as a loading control. Data are presented as mean±SEM. (e) Representative images of IHC staining demonstrated the different expression levels of *INF2* in HCC tissues. Score analysis of IHC staining showed a higher expression of *INF2* in HCC tissues (n=50) than in paratumor tissues (n=50). ns, no significance; *P<0.05; **P<0.01; ***P<0.001. P: paratumor tissue; C: cancer tissue. (f) Survival curves from the TCGA-LIHC cohort showed that HCC patients with high *INF2* have shorter overall survival (P=0.018).

Center in 2021. To expand the sample size and further verify the differences in the expression of *INF2* protein in liver cancer tissues, IHC staining of *INF2* protein was performed in a total of 50 HCC and corresponding paratumor tissues. *INF2* staining showed different shades of brownish yellow and was mainly located in the cytoplasm of HCC and

paratumor tissues, and a small amount was located on the cell membrane. Compared with HCC tissues, *INF2* was weakly expressed or not expressed in the corresponding paratumor tissues. IHC staining results showed that the expression level of *INF2* in HCC tissues could be classified into three types: negative, low positive, and positive. Among the 50 HCC

tissues, 7 (14%) were negative for INF2 expression, 33 (66%) had low expression of INF2, and 10 (20%) were for high expression (positive) for INF2. In HCC tissues, the positive expression rate of INF2 was 86% (43/50), whereas that in paratumor tissues was only 46% (23/50), and the difference was statistically significant. The expression level of INF2 in HCC tissues was significantly higher than that in corresponding paratumor tissues (Figure 1e). Furthermore, the Genomic Data Commons (GDC) TCGA database analysis showed that high INF2 expression was associated with poor HCC prognosis ($P=0.018$) (Figure 1f). Therefore, INF2 may be a highly specific biomarker of HCC.

2.2 The Association of INF2 expression with clinical pathological features of HCC

First, we used UALCAN to analyze the relationship between INF2 transcript expression and various clinical features of HCC. The results showed that *INF2* mRNA in HCC samples was up-regulated in cancer stage 4, nodal metastasis status N1, TP53 mutations, and advanced age (Figure 2a-f). Based on the expression level of INF2 in HCC, we analyzed the correlation between protein expressions of INF2 and clinicopathological features, including patient's gender, age, liver cirrhosis, HBV DNA, α -fetoprotein (AFP) level, differentiation degree, and TNM stage.

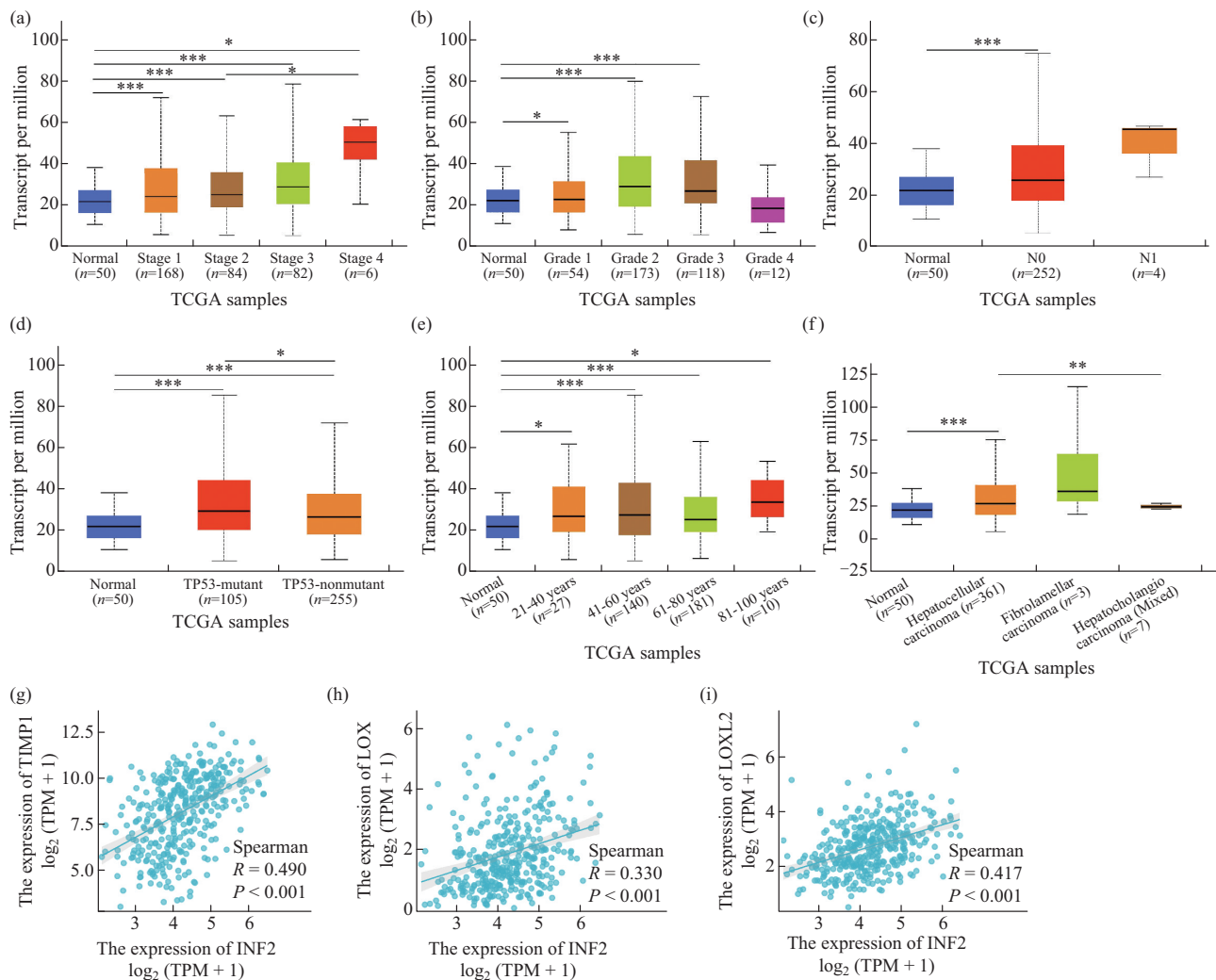


Fig. 2 Expression of INF2 transcription in different clinical characteristics of patients with liver hepatocellular carcinoma (LIHC) via UALCAN

(a) Correlation of INF2 transcription with different cancer stages. (b) Correlation of INF2 transcription with different cancer grades. (c) Correlation of INF2 transcription with different nodal metastasis status. (d) Correlation of INF2 transcription with different TP53 mutation status. (e) Correlation of INF2 transcription with different patient's age. (f) Correlation of INF2 transcription with different histological subtypes. In all panels, * $P < 0.05$; ** $P < 0.01$; *** $P < 0.001$. (g) Correlation of INF2 with TIMP1. (h) Correlation of INF2 with LOX. (i) Correlation of INF2 with LOXL2. TPM: transcript per million.

The comparative method was the chi-square test, and $P < 0.05$. The results are summarized in Table 1. We found that the expression level of INF2 is closely

related to liver cirrhosis ($\chi^2=4.816$, $P=0.041$) and pathological differentiation ($\chi^2=14.579$, $P=0.007$).

Table 1 Association of INF2 expression with clinical pathological features of HCC

Variables	Number	INF2, n (%)			χ^2	P value
		Negative	Low	High		
Gender					2.121	0.176
Male	40	7 (17.5)	25 (62.5)	8 (20.0)		
Female	10	0 (0.0)	8 (80.0)	2 (20.0)		
Age/years					0.173	0.912
<50	10	1 (10.0)	7 (70.0)	2 (20.0)		
≥50	40	6 (15.0)	26 (65.0)	8 (20.0)		
Liver cirrhosis					4.816	0.041
Yes	40	4 (10.0)	26 (65.0)	10 (25.0)		
No	10	3 (30.0)	7 (70.0)	0 (0.0)		
HBV-DNA1					0.737	0.691
Negative	26	4 (15.4)	18 (69.2)	4 (15.4)		
Positive	24	3 (12.5)	15 (62.5)	6 (25.0)		
AFP level/($\mu\text{g}\cdot\text{L}^{-1}$)					0.489	0.780
≤400	32	5 (15.6)	20 (62.5)	7 (21.9)		
>400	18	2 (11.1)	13 (72.2)	3 (16.7)		
Tumor number					0.073	0.789
Single	44	6 (13.6)	29 (65.9)	9 (20.5)		
Multiple	6	1 (16.7)	4 (66.7)	1 (16.7)		
Tumor size/cm					0.183	0.913
≤5	22	3 (13.6)	4 (63.6)	15 (22.7)		
>5	28	4 (14.3)	19 (67.9)	5 (17.9)		
Differentiation					14.579	0.007
Poor	8	0 (0.0)	3 (37.5)	5 (62.5)		
Poor-moderate	9	2 (22.2)	6 (66.7)	1 (11.1)		
Moderate	28	3 (10.7)	21 (75.0)	4 (14.3)		
Moderate-high	5	2 (40.0)	3 (60.0)	0 (0.0)		
Liver capsule invasion					2.240	0.831
Yes	4	0 (0.0)	4 (100.0)	0 (0.0)		
No	46	7 (15.2)	29 (63.0)	10 (21.7)		
Microvascular invasion					0.097	0.952
Yes	28	4 (14.3)	18 (64.3)	6 (21.4)		
No	22	3 (13.6)	15 (68.2)	4 (18.2)		
TNM stage					0.073	0.789
I-II	44	6 (13.6)	29 (65.9)	9 (20.5)		
III-IV	6	1 (16.7)	4 (66.7)	1 (16.7)		

Cirrhosis is a major risk factor for liver cancer. Mitochondrial dysfunction not only runs through the entire process of chronic liver disease, cirrhosis, and liver cancer, but also accelerates the malignant transformation of liver cirrhosis. In liver cirrhosis, irritants such as ischemia, hypoxia, and endotoxemia

can lead to mitochondrial dysfunction, which in turn leads to programmed cell death, death-related inflammation, immune response, fibrosis, and further aggravation of liver cirrhosis. This vicious circle leads to liver cancer^[17]. In view of the correlation between the expression level of INF2 in liver cancer tissues

and cirrhosis, we further verified the relationship between INF2 expression and a series of fibrosis markers through literature review and R language analysis, and found that the expression of INF2 was positively correlated with TIMP1 ($P < 0.001$), LOX ($P < 0.001$) and LOXL2 ($P < 0.001$)^[18](Figure 2g-i). A thorough study of the mechanism by which abnormal INF2 expression in liver cancer induces liver cirrhosis may be helpful for effective anti-fibrosis therapy and prevention of liver cancer.

2.3 Knockdown of INF2 inhibited the proliferation and migration of liver cancer cells *in vitro* may via suppressing the Drp1-mediated mitochondrial fission

To evaluate the role of INF2 in HCC, we

constructed stable INF2 overexpression (INF2-OE, hereafter) and knockdown liver cancer cell lines using the same vector system. Transfection efficiency was detected by WB and RT-qPCR, and shINF2#3 was selected because it had the highest knockdown efficiency (Figure S2).

Colony formation assays showed that colony formation efficiency increased dramatically in INF2 overexpressed liver cancer cells, whereas INF2 knockdown inhibited this effect (Figure 3a). Flow cytometry analysis showed that the proportion change of the G1 phase was not consistent between the two INF2-knockdown liver cancer cell lines compared to the control group. However, the proportion of cells in the G1 phase in the shINF2 group was always higher

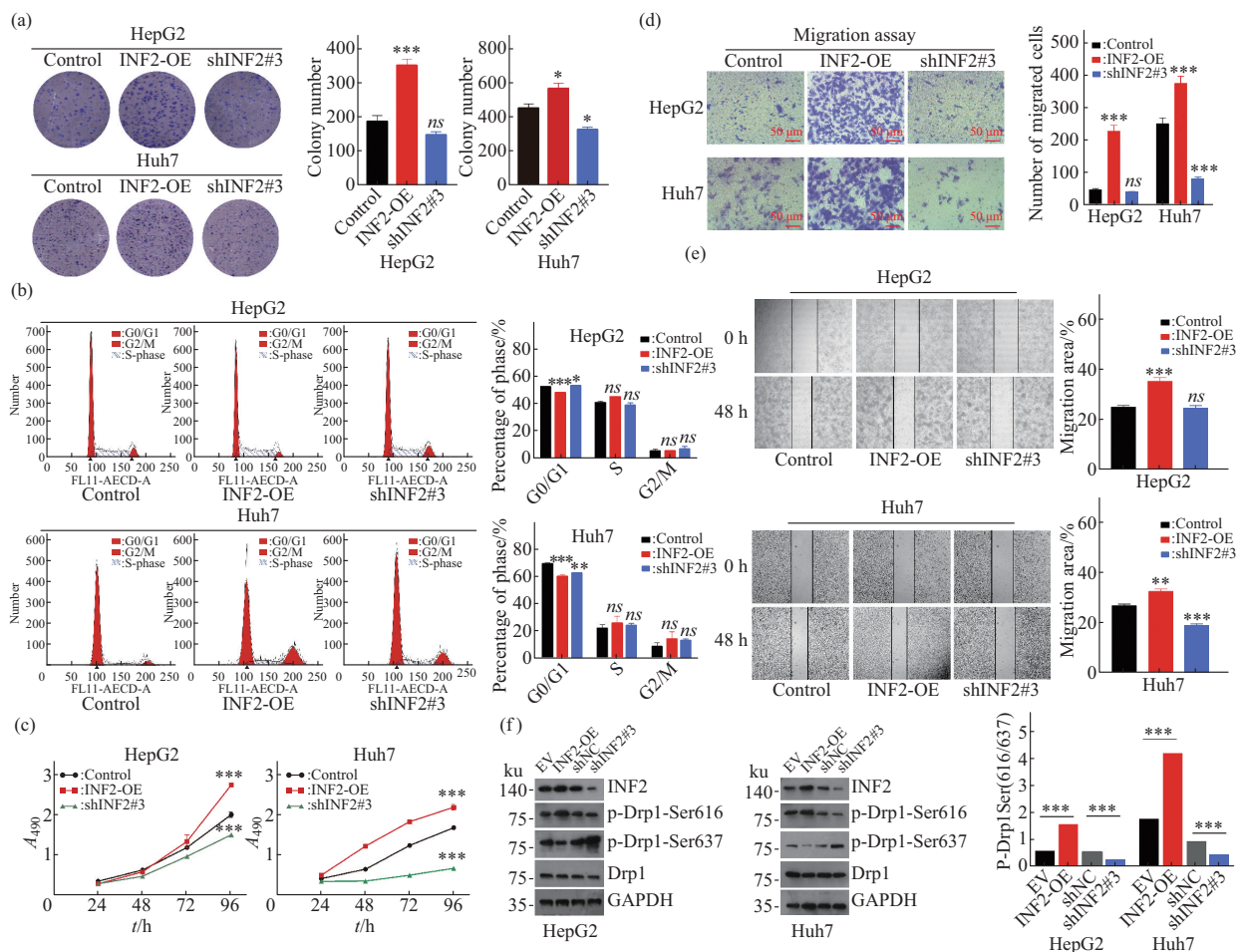


Fig. 3 Effect of INF2 expression on proliferation and migration of hepatoma cells

(a) Colony formation assay showed that overexpression (OE) of INF2 promoted hepatoma cell growth, and shINF2 inhibited the growth of hepatoma cells. (b) Flow cytometry analysis showed that the percentage of the G1 phase decreased in INF2 overexpression cells, which increased in shINF2 cells. (c) Methyl thiazolyl tetrazolium (MTT) assay revealed that cell growth was increased in INF2 overexpression cells, which decreased in shINF2 cells. (d) Migration assay suggested that the migration ability of hepatoma cells was increased after overexpression of INF2, compared to control cells. And the shINF2 decreased the migration ability. (e) Representative micrographs of the wound healing assays. Hepatoma cells were treated with mitomycin C, and cell monolayers were scratched with sterile 200 μ l pipette tips. Images were taken at 0 h and 48 h after scratching. (f) Relationship between INF2 expression level and Drp1 phosphorylation in hepatoma cells. EV, empty vector. Data are presented as mean \pm SEM. In all panels, ns, no significance; * $P < 0.05$; ** $P < 0.01$; *** $P < 0.001$.

than that in the INF2 overexpression group (Figure 3b). MTT assay was used to examine the effect of INF2 expression on the growth of liver cancer cells at different time points. The results revealed that high INF2 expression promoted the growth of liver cancer cells. In contrast, shINF2 inhibited the growth of the liver cancer cells (Figure 3c). Compared with the INF2 overexpressed liver cancer cells, knockdown of INF2 dramatically suppressed the migration of liver cancer cells (Figure 3d, e). A recent study found that aberrantly high expression of INF2 induces the occurrence and progression of endometrial cancer by activating Drp1-mediated mitochondrial hyper-fission by increasing the phosphorylation of Drp1-Ser616 and decreasing the phosphorylation of Drp1-Ser637^[15]. Consistent with these findings, we also found similar results in INF2 overexpressed liver cancer cell lines (Figure 3f).

2.4 INF2 facilitates the growth of liver cancer cells *in vivo*

To further confirm the proliferation promoting role of INF2 in HCC *in vivo*, we utilized *in vivo* xenograft assay to evaluate the effects of INF2 overexpression and knockdown on the growth of HCC growth. Huh7 cells stably expressing control, INF2-OE, or shINF2#3 were injected subcutaneously into nude mice. Tumor size was monitored every 4 d after cell injection. Twenty days after the tumor transplantation, the mice were euthanized. Then, the tumors were dissected, weighed and photographed (Figure 4a). The results showed a significant reduction in tumor volume and mass in the INF2 knockdown group compared to the control group. In contrast, tumor volume and weight increased significantly in the INF2 overexpression group (Figure 4b, c).

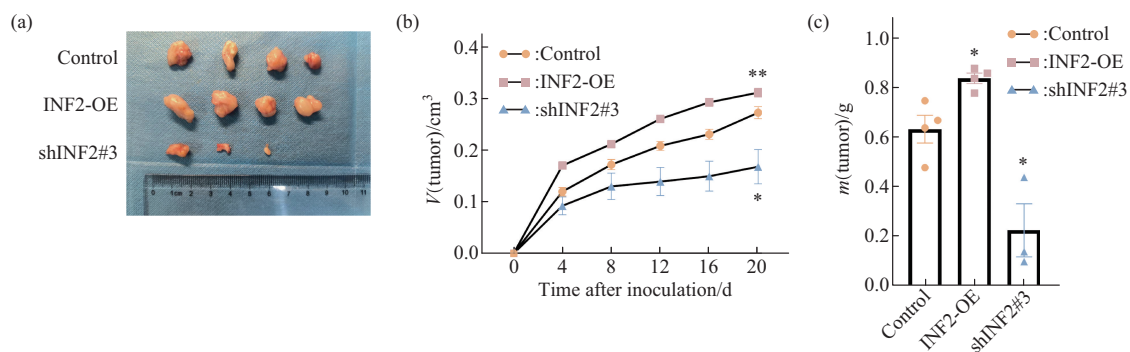


Fig. 4 INF2 facilitates the growth of HCC *in vivo*

(a) Huh7 cells with stable expression of control, INF2-OE, or shINF2#3 were transplanted into female athymic nude mice. Tumors were stripped out and photographed 20 d later. (b) Tumor is measured with a ruler every 4 d, and the tumor volume was calculated using the formula: $V=(\text{length} \times \text{width}^2) \times 1/2$. (c) The tumors were weighed. Data are presented as mean \pm SEM.

2.5 The diagnostic value of INF2 in HCC

To explore the diagnostic value of INF2 in HCC, the receiver operating characteristic curve (ROC) was mapped. INF2 was highly accurate in predicting the prognosis of HCC ($AUC=0.660$, $CI=0.597-0.722$, Figure 5a), pathological differentiation ($AUC=0.705$, $CI=0.528-0.882$, Figure 5d). The ability to predict the prognosis of liver fibrosis and prothrombin time was poor (Figure 5e, f). These results show that INF2 has predictive value for the diagnosis and staging of HCC (Figure 5).

2.6 INF2 expression associated with tumor immunity in HCC

Mitochondrial fission induces immune escape in solid tumors by decreasing MHC-I surface expression. Furthermore, inhibition of mitochondrial fission with Mdivi-1 upregulates MHC-I expression in cancer cells and enhances the efficacy of adoptive T-cell therapy in patient-derived tumor models^[19]. Given the immune tolerance and treatment resistance of clinical HCC treatment, we further explored the relationship between INF2 expression and immune-

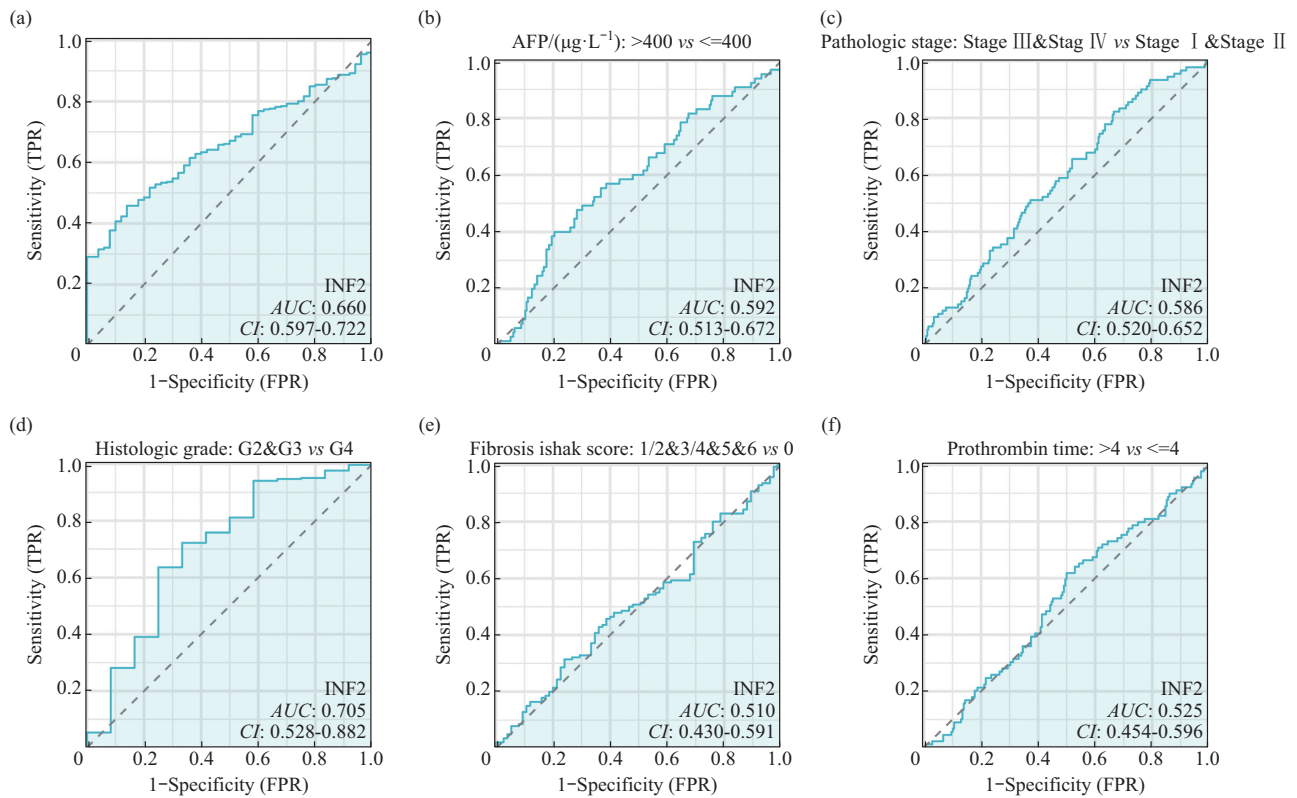


Fig. 5 ROC curve analysis was performed to evaluate the predictive value of INF2 in HCC

(a) ROC curve analysis was performed to evaluate the predictive value of INF2 for HCC diagnosis. (b) ROC curve analysis was performed to evaluate the predictive value of INF2 for AFP status. (c) ROC curve analysis was performed to evaluate the predictive value of INF2 for pathologies. (d) ROC curve analysis was performed to evaluate the predictive value of INF2 for histologic grade. (e) ROC curve analysis was performed to evaluate the predictive value of INF2 for fibrosis ishak score. (f) ROC curve analysis was performed to evaluate the predictive value of INF2 for prothrombin time. TPR: true positive rate; FPR: false positive rate.

related signals. TIMER2.0 database was used to analyze INF2 mRNA expression and the six categories of immune cells. The results revealed that *INF2* mRNA expression positively correlated with B cells ($R=0.194, P<0.001$), CD4+T cells ($R=0.315, P<0.001$), macrophages ($R=0.286, P<0.001$), neutrophils ($R=0.360, P<0.001$), and dendritic cells (DCs) ($R=0.356, P<0.001$) (Figure 6a). Subsequently, we further investigated the connection between the *INF2* gene level and the degree of 24 immune cells infiltration using ssGESA. The results demonstrated that *INF2* mRNA expression was positively correlated with NKCD56bright cells ($R=0.403, P<0.001$), macrophages ($R=0.305, P<0.001$), T cells ($R=0.142, P<0.01$), TH1 cells ($R=0.117, P<0.05$), TH2 cells ($R=0.108, P<0.05$) (Figure 6b). This is similar to the results of the Timer database. In addition, the R language platform was used to analyze the correlation

between the expression levels of INF2 and PD-L1 in hepatocellular carcinoma in the TCGA database, and it was found that INF2 was positively correlated with PD-L1 expression (Figure 6c). Similarly, IHC analysis of 50 clinical HCC tumor samples showed that INF2 expression levels were positively correlated with PD-L1 at the protein levels ($R=0.4423, P<0.01$) (Figure 6d). Therefore, we speculate that INF2, as a carcinogenic protein in HCC, may up-regulate PD-L1 and down-regulate MHC-I expression by regulating mitochondrial fission, resulting in a poor prognosis of HCC. The specific mechanism remains to be further studied (Figure 6e). The cross-talk between mitochondrial dynamics disorders and tumor immunity suggests that combining mitochondrial fission inhibitors with immunotherapy may have unexpected effects.

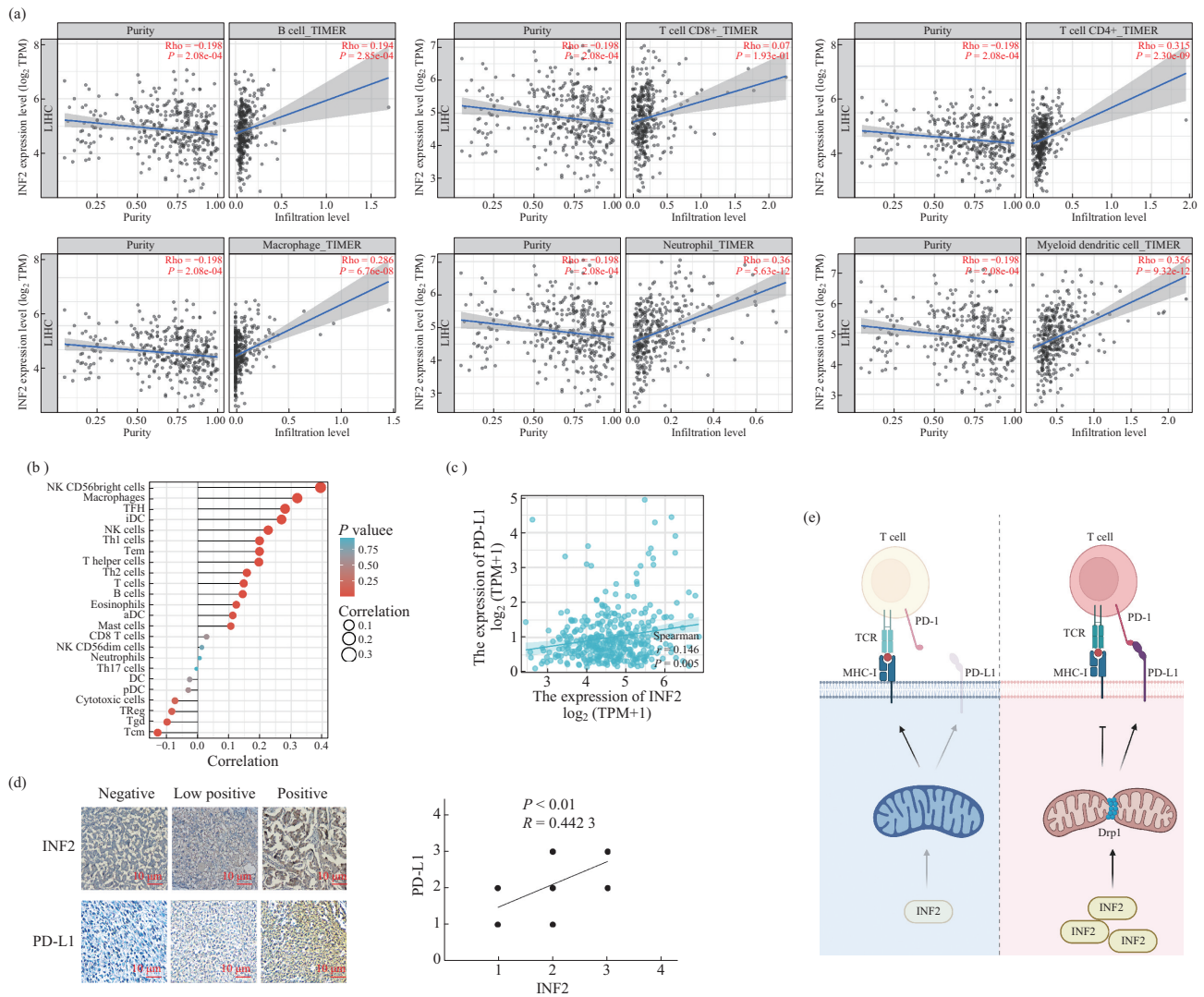


Fig. 6 The correlation between INF2 expression level and tumor immunity

(a) INF2 expression is associated with immune cell infiltration. (b) The expression level of INF2 was positively correlated with the infiltration level of Th1 lymphocytes, Th2 lymphocytes, T cells, B cells, and other immune cells. (c) INF2 was positively correlated with PD-L1. (d) Representative IHC images of INF2 and PD-L1 in HCC tissues ($n=50$). The correlation analysis of INF2 and PD-L1 staining in HCC tissues ($P < 0.01$). (e) Potential work model of elevated INF2 in HCC. TPM: transcript per million.

3 Discussion

Although accumulating evidence indicates that the crosstalk between liver cancer cells and mitochondrial dynamic fusion and fission plays a vital role in HCC occurrence and progression^[20-23], the underlying mechanism of this crosstalk and the unique target to mitochondrial dynamic fusion and fission in HCC are not completely known. Here, we demonstrated that the mitochondrial fission related protein INF2, is significantly overexpressed in HCC samples from TCGA data and clinical HCC patients'

tissues, resulting in poor survival and low pathological differentiation. Moreover, upregulated INF2 promoted the proliferation and migration of liver cancer cells, which was inhibited by shINF2. Therefore, our results suggest that a specific target of INF2 may be a potential treatment strategy for patients with HCC with high INF2 expression.

Structurally, INF2 is a member of the formin family, which function is as an actin assembly factor. Therefore, INF2 has multiple effects on actin polymerization, as well as having both direct or indirect effects on microtubule dynamics, playing

roles in cytokinesis, cell motility, mitochondrial fission, ER-to-mitochondrial calcium transfer, vesicle trafficking, and Golgi structure^[10-11]. Intriguingly, compared to its detailed downstream function, the upstream regulation of INF2 is limited. One well-known regulation is the autoinhibited regulatory model *via* the interaction of its own N-terminal domain DID and DAD^[11]. One previous study found that the post-translational modification of INF2, SPOP-mediated non-degradative ubiquitination, reduces INF2 localization in the ER and thus abrogates its ability to facilitate mitochondrial fission^[12]. Recently, another related study found that FBXO7 acts as a tumor suppressor in endometrial cancer by inhibiting the INF2-Drp1 axis, which is associated with mitochondrial fission through ubiquitination and degradation of INF2. Drp1 phosphorylation regulates mitochondrial dynamics that Drp1 Ser616 phosphorylation promotes mitochondrial fission, while Drp1 Ser637 phosphorylation has the opposite^[15]. Herein, we found that the proportion of Drp1 Ser616/637 increased in the INF2 overexpression group, but decreased in the INF2 knockdown group (Figure 3f). Therefore, INF2 in liver cancer cells may affect mitochondrial fission by recruiting Drp1 or inducing Drp1 phosphorylation, thereby promoting tumor progression.

The correlation between INF2, mitochondrial dynamics and tumor immunity suggests that the INF2-related signal in HCC should be detected, and further studies are required. Given the efficacy of suppression of INF2 and that there is no molecular compound targeting INF2, we suggest high-throughput screening of compounds using gene expression modulation by small molecules (GEMS) technology, where reduced luciferase INF2 reporter activity was measured to identify compounds that lower INF2 transcript levels. Thus, the efficiency of selected compounds in inhibiting INF2 in different cancer cell models need to be determined. In addition, E3 ligase targeting to INF2, which is responsible for its degradation, is also urgent to be found by the method of yeast two-hybrid or affinity purification and mass spectrometry (AP-MS). Additionally, it may be an effective way to find the special miRNA targeting INF2 by using miRNA microarray analysis.

4 Conclusion

In conclusion, INF2 is abnormally highly expressed in HCC and is associated with liver fibrosis, poor tumor differentiation, and even poor prognosis. High expression of INF2 promotes HCC proliferation *in vivo* and *in vitro*, which may be achieved by inducing Drp1 phosphorylation and upregulating PD-L1 expression. Targeting INF2 may be a potential therapeutic strategy for HCC, and further studies are needed to confirm it in the future.

Supplementary Available online (<http://www.pibb.ac.cn>, <http://www.cnki.net>):

PIBB_20240151_Figure_S1.pdf

PIBB_20240151_Figure_S2.pdf

References

- [1] Bray F, Laversanne M, Sung H, *et al.* Global cancer statistics 2022: GLOBOCAN estimates of incidence and mortality worldwide for 36 cancers in 185 countries. *CA Cancer J Clin*, 2024, **74**(3): 229-263
- [2] Llovet J M, Kelley R K, Villanueva A, *et al.* Hepatocellular carcinoma. *Nat Rev Dis Primers*, 2021, **7**(1): 6
- [3] Singal A G, Ng M, Kulkarni A. Advancing surveillance strategies for hepatocellular carcinoma: a new era of efficacy and precision. *J Clin Exp Hepatol*, 2024, **14**(6): 101448
- [4] Chidambaranathan-Reghupaty S, Fisher P B, Sarkar D. Hepatocellular carcinoma (HCC): epidemiology, etiology and molecular classification. *Adv Cancer Res*, 2021, **149**: 1-61
- [5] Xiang L, Shao Y, Chen Y. Mitochondrial dysfunction and mitochondrion-targeted therapeutics in liver diseases. *J Drug Target*, 2021, **29**(10): 1080-1093
- [6] Hu J, Zhang H, Li J, *et al.* ROCK1 activation-mediated mitochondrial translocation of Drp1 and cofilin are required for arimidiol-induced mitochondrial fission and apoptosis. *J Exp Clin Cancer Res*, 2020, **39**(1): 37
- [7] Kraus F, Roy K, Pucadyil T J, *et al.* Function and regulation of the divisome for mitochondrial fission. *Nature*, 2021, **590**(7844): 57-66
- [8] Tabish T A, Narayan R J. Mitochondria-targeted graphene for advanced cancer therapeutics. *Acta Biomater*, 2021, **129**: 43-56
- [9] Fung T S, Chakrabarti R, Higgs H N. The multiple links between actin and mitochondria. *Nat Rev Mol Cell Biol*, 2023, **24**(9): 651-667
- [10] Labat-de-Hoz L, Alonso M A. The formin INF2 in disease: progress from 10 years of research. *Cell Mol Life Sci*, 2020, **77**(22): 4581-4600

- [11] Zhao Y, Zhang H, Wang H, *et al.* Role of formin INF2 in human diseases. *Mol Biol Rep*, 2022, **49**(1): 735-746
- [12] Jin X, Wang J, Gao K, *et al.* Dysregulation of INF2-mediated mitochondrial fission in SPOP-mutated prostate cancer. *PLoS Genet*, 2017, **13**(4): e1006748
- [13] Heuser V D, Mansuri N, Mogg J, *et al.* Formin proteins FHOD1 and INF2 in triple-negative breast cancer: association with basal markers and functional activities. *Breast Cancer*, 2018, **12**: 1178223418792247
- [14] Heuser V D, Kiviniemi A, Lehtinen L, *et al.* Multiple formin proteins participate in glioblastoma migration. *BMC Cancer*, 2020, **20**(1): 710
- [15] Zhang H, Zhao Y, Wang J, *et al.* FBXO7, a tumor suppressor in endometrial carcinoma, suppresses INF2-associated mitochondrial division. *Cell Death Dis*, 2023, **14**(6): 368
- [16] Qian J, Fang D, Lu H, *et al.* Tanshinone IIA promotes IL2-mediated SW480 colorectal cancer cell apoptosis by triggering INF2-related mitochondrial fission and activating the Mst1-Hippo pathway. *Biomed Pharmacother*, 2018, **108**: 1658-1669
- [17] Chu Q, Gu X, Zheng Q, *et al.* Mitochondrial mechanisms of apoptosis and necroptosis in liver diseases. *Anal Cell Pathol (Amst)*, 2021, **2021**: 8900122
- [18] Dhar D, Baglieri J, Kisseleva T, *et al.* Mechanisms of liver fibrosis and its role in liver cancer. *Exp Biol Med (Maywood)*, 2020, **245**(2): 96-108
- [19] Lei X, Lin H, Wang J, *et al.* Mitochondrial fission induces immunoescape in solid tumors through decreasing MHC-I surface expression. *Nat Commun*, 2022, **13**(1): 3882
- [20] Li M, Wang L, Wang Y, *et al.* Mitochondrial fusion *via* OPA1 and MFN1 supports liver tumor cell metabolism and growth. *Cells*, 2020, **9**(1): 121
- [21] Yu Y, Peng X D, Qian X J, *et al.* Fis1 phosphorylation by Met promotes mitochondrial fission and hepatocellular carcinoma metastasis. *Signal Transduct Target Ther*, 2021, **6**(1): 401
- [22] Hernández-Alvarez M I, Zorzano A. Mitochondrial dynamics and liver cancer. *Cancers*, 2021, **13**(11): 2571
- [23] Che L, Wu J S, Du Z B, *et al.* Targeting mitochondrial COX-2 enhances chemosensitivity *via* Drp1-dependent remodeling of mitochondrial dynamics in hepatocellular carcinoma. *Cancers*, 2022, **14**(3): 821

倒立式蛋白2 (INF2) 高表达预示不良预后 并促进肝细胞癌进展*

王海彪^{1)**} 林 纁^{3)**} 叶扶桑⁴⁾ 石佳鑫³⁾ 李 宏^{1,3)***} 叶 孟^{2,3)***} 汪 洁^{2)***}

¹⁾ 宁波市医疗中心李惠利医院肝胆胰外科, 宁波 315040;

²⁾ 宁波大学附属第一医院放化疗科, 宁波 315010;

³⁾ 宁波大学生物化学与分子生物学实验室, 浙江省病理生理学技术研究重点实验室, 科学健康中心, 宁波 315211;

⁴⁾ 宁波市临床病理诊断中心病理科, 宁波 315021)

摘要 目的 INF2 是 formins 蛋白家族的一员, INF2 的异常表达和调控与多种肿瘤进展有关, 但 INF2 在肝细胞癌 (hepatocellular carcinoma, HCC) 中的表达及作用仍不清楚。HCC 是高度致命的恶性肿瘤, 鉴于传统治疗的局限性, 为寻求新的治疗靶点, 本研究探索了 INF2 在 HCC 中的表达水平、临床价值及潜在作用机制。**方法** 本研究利用公共数据库分析了 INF2 在泛癌及 HCC 中的表达情况及 INF2 表达水平对 HCC 预后的影响。采用实时定量 PCR (quantitative real time polymerase chain reaction, RT-qPCR)、蛋白质印迹技术、免疫组化检测了 INF2 在 HCC 细胞及人 HCC 组织中的表达水平。利用公共数据库及人 HCC 标本临床数据分析了 INF2 表达与临床病理特征的相关性。随后, 通过体外和体内实验阐明了 INF2 表达水平对 HCC 细胞生物学功能及 Drp1 磷酸化的影响。最后, 通过数据库和免疫组化实验, 进一步分析了 INF2 在 HCC 中的预测价值及潜在作用机制。**结果** INF2 在 HCC 中异常高表达, 且 INF2 高表达与 HCC 患者总生存期、肝硬化和病理分化相关。INF2 表达水平在预测 HCC 预后及病理分化程度上有一定的诊断价值。在体内外 HCC 模型中, INF2 的表达上调会触发 HCC 细胞的增殖和迁移, 而 INF2 的敲除可以抵消这种作用。HCC 细胞中的 INF2 可能通过诱导 Drp1 磷酸化影响线粒体分裂, 并上调 PD-L1 的表达介导免疫逃逸, 进而促进肿瘤进展。**结论** INF2 在 HCC 中高表达并与不良预后相关。INF2 高表达可能通过诱导 Drp1 磷酸化及 PD-L1 表达上调促进 HCC 进展, 靶向 INF2 可能对高表达 INF2 的 HCC 患者有利。

关键词 肝细胞癌, 倒立式蛋白2 (INF2), 表达, 预后, Drp1

中图分类号 R735.7

DOI: 10.16476/j.pibb.2024.0151

CSTR: 32369.14.pibb.20240151

* 宁波市自然科学基金 (202003N4197), 宁波市卫生健康科技计划 (2022Y13), 宁波市消化系统肿瘤临床医学研究中心 (2019A21003), 浙江省基础公益研究计划 (LTGY24H160004), 浙江省医药卫生计划 (2022KY1079), 宁波市大学生科研创新计划 (2024SRIP1925) 和宁波大学王宽诚基金资助项目。

** 并列第一作者。

*** 通讯联系人。

李宏 Tel: 0574-87018651, E-mail: lancet2017@163.com

叶孟 Tel: 0574-87085337, E-mail: yemeng@nbu.edu.cn

汪洁 Tel: 0574-87085337, E-mail: wangjiemedical@163.com

收稿日期: 2024-04-09, 接受日期: 2024-08-29